JOURNAL OF MATERIALS SCIENCE **33** (1998) 3623–3628

Positron annihilation in hydrogenated YBCO superconductor

W. M. CHEN*, S. S. JIANG, L. Y. LI, K. SHEN, X. S. WU, X. JIN
Department of Physics and National Laboratory of Solid State Microstructure, Nanjing University, Nanjing 210093, People's Republic of China
E-mail: wmchen@nju.edu.cn

Y. C. GUO, X. S. DOU
Centre for Superconducting and Electronic Materials, University of Wollongong, Wollowong, New South Wales 2522, Australia

H. O. XIONG, L. W. SHAO
Analysis and Test Centre, Southeast University, Nanjing, People's Republic of China

The behaviour of hydrogenated $YBa_2Cu_3O_y$(YBCO) has been investigated by sputtering neutral-particle mass spectrometry (SNMS) and positron annihilation lifetime spectrum analysis. SNMS analysis shows that hydrogen in YBCO is in the covalent form. In order to interpret experimental results, a hydrogenation model is suggested in which hydrogen occupies sites H_1, H_2 and H_3 where H_1 is in the CuO chains and H_2 and H_3 are in the plane occupied by Y. To study the two positron annihilation lifetimes τ_1 and τ_2, the electronic densities in special "rooms" the unit cell of YBCO, which are relative to H_1, H_2 and H_3 were calculated. The results show that the process of τ_1 occurs in the "room" where barium is located, and that of τ_2 is decided by the hydrogen occupied sites H_2 and H_3. The variation of τ_2 following hydrogenation is considered to be a result of hydrogen occupying H_2 and then diffusing to H_1. © *1998 Kluwer Academic Publishers*

1. Introduction

Superconductivity has been studied and a series of results has recently been published [1–7]. However, some problems remain, especially the important point concerning the location of hydrogen [8]. In general, X-ray analysis is a powerful method to determine crystal structures and the probabilities of some sites being occupied by elements. Unfortunately, the analysis is not adequate for light elements, such as hydrogen. In order to deal with this problem, sputtering neutral-particle mass spectrometry (SNMS) experiments have been undertaken to determine the hydrogen valence, and positron annihilation lifetime spectroscopy (PALS) was used to decide the attribution of vacancies and their changes during hydrogenation. To interpret the experimental results, a model of hydrogen atoms occupying some sites and then diffusing to other sites, has been postulated. Using this model, the main experiment results of SNMS and PALS can be explained.

2. Experimental procedure

2.1. Experiment 1

Samples of YBCO were prepared by a solid reaction method. Raw materials of CuO, Y_2O_3 and $BaCO_3$ in the ratio stoichiometric of 1 : 2 : 3 were mixed, ground and preheated at 930 °C for 24 h in air, then furnace cooled. The reactants were then ground and preheated again. After being ground and pressed into flats (samples), samples were heated at 930 °C for 24 h in flowing oxygen. Then the heating procedures were divided into two steps: one for the quenched sample and the other for the annealed one. The quenched sample was rapidly quenched from 930 °C to room temperature. For the annealed sample, the heating temperature was reduced from 930 °C to 350 °C at a speed of 1 °C min^{-1} held 350 °C for 24 h, and then the sample was cooled to room temperature in the furnace. The structures of the annealed and quenched samples were characterized by X-ray powder diffraction analysis as orthorhombic and tetragonal phases, respectively.

The average valence of copper, $2 + p$, and the oxygen content, y, were determined by an improved double iodometric titration [9]. Instead of the traditional one, a new equation was adopted to calculate p [10]

$$p = [(V_1/M_1)/(V_2/M_2) - 1]/[1 - 8CV_1/M_1] \quad (1)$$

where M(g) is the mass of the sample; V(ml) and C (mol ml^{-1}) are the volume and concentration of the $Na_2S_2O_3$ solution used, respectively; and subscripts

---

*Author to whom all correspondence should be addressed.

represent the first and second titrimetric experiments, respectively. As a comparison, the traditional equation is [11]

$$p = (V_1/M_1)/(V_2/M_2) - 1 \qquad (2)$$

which is a simpler but less accurate one. From the theorem of charge neutrality, the dependence of the oxygen content of YBCO, y, on p can be expressed as $y = 6.5 + 1.5p$. The value of the oxygen content of the orthorhombic sample was 6.886 and that of the tetragonal phase was 6.401. Measurements of electrical resistivity were carried out on samples using the four-ends method. For the orthorhombic phase, the superconducting critical temperature with zero resistance, T_c, was 91.4 K, and after hydrogenation $T_c = 86.0$ K.

2.2. Experiment 2

Samples were put in a chamber containing dry, pure, and flowing hydrogen gas with a pressure of 10^4 Pa. The hydrogenation was performed at room temperature for 10, 40, 100, 220, 460, 1000, 1960, 3400, and 6280 min.

After hydrogenation, SNMS analysis was carried out using a type QS-250 SNMS spectrometer operating from 2–250 atomic mass units (a.m.u). Its resolution reaches $\Delta M \leqslant 1$ a.m.u., and the sensitivity is 10 p.p.m. for trace element analysis. The sputtering time in this experiment lasted for 1500 s. Relative hydrogen content and bond state in YBCO were determined, as shown in Fig. 1.

2.3. Experiment 3

Positron annihilation experiments were performed for various hydrogenated samples with the fast–fast coincidence method using a typical positron lifetime spectrometer. A radioactive source of ^{22}Na was used as the positron source. PALS was performed according to standard regulations described elsewhere [12]. The resolution function of the positron lifetime spectrometer was 370 ps. Each datum of PALS of lifetime was recorded when the number of γ-ray counts equalled or exceeded 10^6. The recorded lifetime spectrum was a multi-exponential function. It was resolved into three components by a least squares fit. The component with the smallest intensity had no influence on the behaviour of the samples, determined by the positron source. The discussion below is based on the other two components, named τ_1 and τ_2. The average positron annihilation lifetime, τ, may be expressed as

$$\tau = I_1\tau_1 + I_2\tau_2 \qquad (3)$$

where I_1 and I_2 are relative intensities of τ_1 and τ_2, respectively, i.e. $I_1 + I_2 = 1$. For samples with orthorhombic and tetragonal phases, the values of τ, I_2 and τ_2 are shown in Figs 2 and 3.

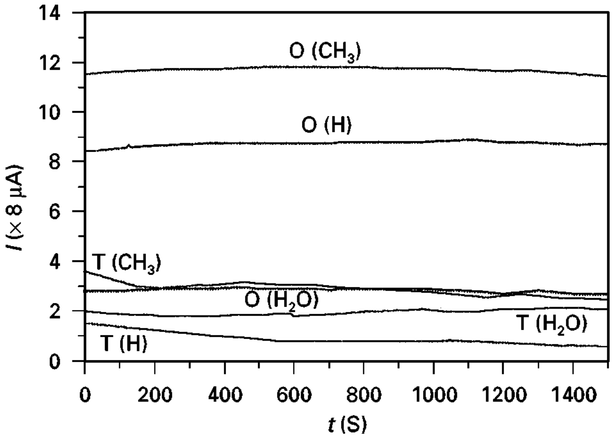

Figure 1 A plot of the intensity of sputtering electric current, I, against the sputter time, t. O and T represent orthorhombic and tetragonal samples of YBCO, respectively. In the SNMS experiment, hydrogen can be found in three forms: H, H_2O, and CH_3. For the orthorhombic sample, the intensity of CH_3 is four times that of H_2O.

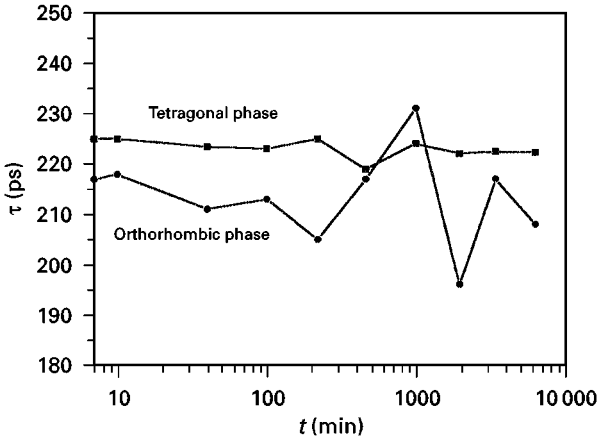

Figure 2 The average positron annihilation lifetime, τ versus hydrogenating time, t. τ in the tetragonal sample is almost constant during hydrogenation, but that of the orthorhombic sample varies with hydrogenation.

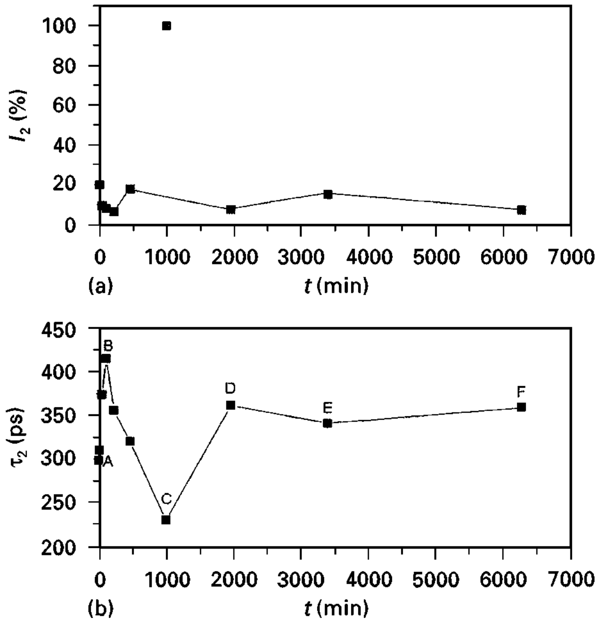

Figure 3 (a) The intensity and (b) the lifetime of the second component of PALS as a function of hydrogenating time for the orthorhombic sample.

3. Model of the hydrogenating process

3.1. The form of hydrogen in YBCO

We were interested in how many hydrogen molecules can enter a unit cell of YBCO and which sites they occupy. To find the answer, Fig. 1 was analysed and two facts were discovered. First, hydrogen can enter cells of both orthorhombic and tetragonal phases, with different valence. Second, the average positron annihilation lifetime of the tetragonal phase, τ, is almost constant, and the quantities of hydrogen entering into a tetragonal sample are much smaller than the quantities of those entering an orthorhombic one, as shown in Fig. 1. Therefore, we concentrated on the study of the orthorhombic phase.

In Fig. 1, both hydrogen and hydrogenates exist at different depths in YBCO. H represents a form of dissociated hydrogen, which is absorbed on crystal boundaries or on defects in grains and does not enter the unit cell or combine with other elements. The existence of H_2O is unusual, because no water enters YBCO during synthesis of YBCO or during the hydrogenizing procedures. There are two ways to interpret this fact. The direct explanation is that hydrogen takes oxygen from YBCO and they combine to form water. As is known, in CuO_2 planes there are many oxygen atoms which are stable. Even at a high temperature, no oxygen cavities can be found in CuO_2 planes of tetragonal YBCO. Therefore, oxygen cannot escape from CuO_2 planes. Let us consider the oxygen in CuO chains. It is easy for oxygen to enter into or depart from these sites along the *b*-axis. If some oxygen atoms in the *b*-axis are lost, the carrier concentration will decrease, and a structure transition from superconducting orthorhombic to non-superconducting tetragonal phase will occur. However, in this case, no change of T_c was observed [7]. Researchers also believed that hydrogen did not take oxygen from YBCO but entered into it [7, 8]. In our experiment, T_c decreased to 86 K, but the sample was still in the superconducting phase. Therefore, we do not consider the existence of water to be the result of hydrogen taking oxygen from YBCO. Even if the reaction of hydrogen combining with oxygen occurs at room temperature, it is certain that the reaction is not the major source of H_2O, because the amount of the oxygen in the superconducting phase is not evidently reduced after hydrogenation. So we seek another interpretation: the appearance of H_2O is the result of hydrogen occupying some sites surrounded by oxygen. When the hydrogen occupies these sites, hydrogen–oxygen bonds are formed in hydrogenized YBCO and behave like H_2O in the SAMS experiment. We note that the values of the *a* lattice constant were obviously increasing, but that of *b* remained constant during the beginning of the hydrogenized period [7]. Therefore, hydrogen ions can be considered to occupy sites of (1/2, 0, 0) surrounded by two copper and eight oxygen atoms, as shown in Fig. 4.

In CH_3, the C–H bond is covalent. We notice that CH_3 appears not only on the surface but also at all sputtered depths. However, no carbonate was added to the YBCO during preparation and hydrogenation of the samples. Even if there is contamination with carbonate, it will be on the surface only, not at the all sputtered depths. So the appearance of CH_3 can only be explained as a covalent bond existing when hydrogen ions occupy some sites of YBCO. In this analysis, carbon is actually a substitution for yttrium, the only element having a valency of 3 in the family III_B of the Periodic Table in our sample, and whose data are not available in SAMS. Therefore, we conclude that hydrogen "combines" with yttrium in the state of a covalent bond. In other words, for hydrogenated YBCO, hydrogen atoms appear in the place where yttrium is located.

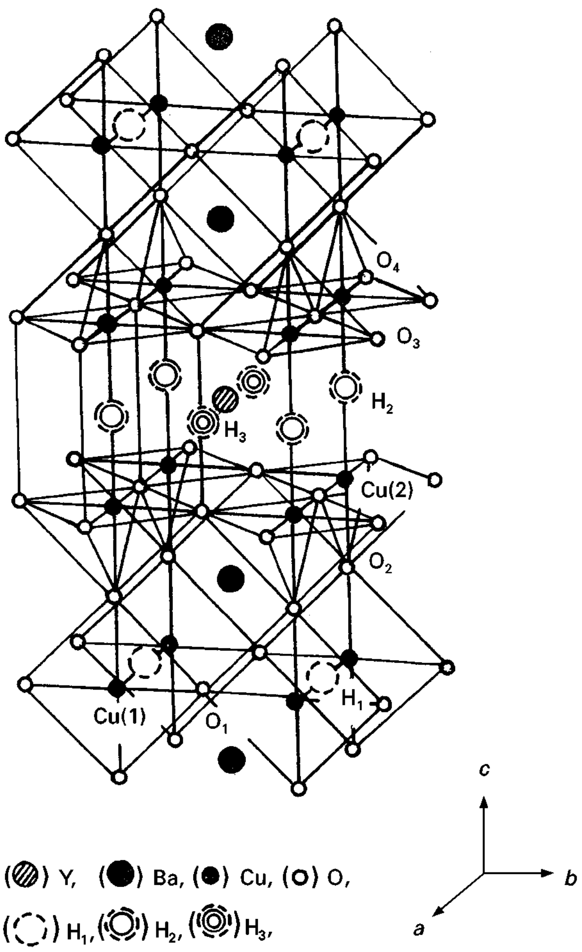

Figure 4 The model of hydrogenated YBCO and its sites of H_1, H_2 and H_3.

3.2. Model of hydrogen occupying some sites of YBCO

According to the experiment results, we can suggest a model for hydrogenated YBCO: three kinds of sites in the unit cell of YBCO, (1/2, 0, 0) named H_1, (0, 0, 1/2) named H_2, (0, 1/2, 1/2) or (1/2, 0, 1/2) named H_3, can be occupied by hydrogen, as shown in Fig. 4. In the H_2 site, each hydrogen ion is surrounded by four yttrium ions, but no CH_4 appears in the SAMS results. Thus, it is necessary for more hydrogen to enter into the "room" in which yttrium is located. The sites left in this "room" are H_3. There are four sites in a cell for H_3. If all of those are occupied by hydrogen, the state of valence would show in the form of CH_2. However, the SAMS results show the state of valence to be in the form of CH_3 instead of CH_2. If two of them are occupied by hydrogen, the probability of occupation of H_3 is 0.5. Thus, in this model, H_2 and H_3 sites occupied by hydrogen in the yttrium plane are similar to those sites at the Cu(1) plane occupied by oxygen.

4. Positron annihilation lifetime experiments and discussion

4.1. Probability of the appearance of positrons

The average lifetime of positron annihilation, τ, may provide information about the whole state of the microstructure of YBCO and it depends on the average electronic density of the crystal in the sample. In a square-well potential, τ can be given by [13].

$$\tau = 1/\pi r_0^2 cnp \tag{4}$$

where r_0, n and c are, respectively, the electronic classical radius, the electronic density and the speed of light; p is the probability of finding positronium outside the square-well where positron or positronium annihilate. If we take each unit cell as a square well, τ on the left-hand side of Equation 4 will express the average positron annihilation lifetime. Because τ has been measured in experiment 3, the average p of YBCO can be calculated from Equation 4. For virgin YBCO with orthorhombic and tetragonal phases, the calculated results are listed in Table I.

In the last column of Table I, the tetragonal p to orthorhombic p ratio is about 1.02. Therefore, the probabilities of positronium or positron appearing in the region of a crystal cell for both orthorhombic and tetragonal phases are similar, but the former is greater than the latter by 2%.

4.2. Calculated electronic densities

In order to calculate positron annihilation lifetime, the electronic densities of vacancies or bivacancies in the cell of YBCO are calculated as follows. We divide the unit cell of orthorhombic YBCO into two "rooms": one is a "room" with a barium atom in the centre, the other is a "bivacancy" with an yttrium atom in the centre. Bariums "room" consists of three parts. They are: monovacancy with an H_1 site in the centre, a pyramid of Cu–O in the corner of the "room" and the vacancy and a horizontal square bar with a barium in the centre. The monovacancy of H_1 has two copper neighbours, and each copper is surrounded by four oxygen atoms. The Cu–O pyramid consists of five oxygen atoms and one copper atom, in which four oxygen atoms form a square bottom, the fifth one is at the top of the pyramid, and the copper locates in the centre near the bottom. The square bar of barium, surrounded by eight oxygen atoms, has two bottoms with the length of the a lattice constant between. The "room" in which yttrium is located is a bivacancy, as shown in Fig. 4. One vacancy consists of eight oxygen atoms in the form of a vertical square bar, with H_2 in the centre, the other vacancy is also a vertical square bar surrounded by eight oxygen atoms but with an yttrium atom in the centre.

For convenience of calculation, sites of Cu(2), O(3) and O(4) are considered to be in the same plane determined by the average of their coordinative values, i.e. $z = 0.3665c$. For all the above vacancies, calculated results are listed in Table II. The number of monovacancies, vacancies and pyramids are listed in the second column. Their volumes in unit cell volume and in nm^3 are listed in the third and fourth columns. The fifth column corresponds to the elements they possess, with the number in parentheses indicating the sites of those elements. The total electronic number

TABLE I Electronic number, N, and density n, calculated for a YBCO cell, based on $a = 0.382$ nm, $b = 0.388$ nm, $c = 1.169$ nm and $a = b = 0.387$ nm, $c = 1.172$ nm for orthorhombic and tetragonal phases, respectively. The average lifetime of positron annihilation, τ, is determined in the positron annihilation experiment. The mean probability, p, of positronium or positron appearance around the crystal cell is calculated from Equation 4

YBCO	Cell volume, V (nm^3)	Electronic number, N	Electronic density, n(nm^{-3})	Lifetime, τ (ps)	Probability of positron, p
Orthorhombic	0.173	294	1699	215	0.367
tetragonal	0.175	290	1657	225	0.360
O-to-T ratio	0.99:1	1.014:1	1.025:1	0.956:1	1.019:1

TABLE II Volumes, number of elements and electrons, electron density, and corresponding positron annihilation lifetime are calculated for all orthorhombic YBCO vacancies

Name	N	V(cell)	V(nm^3)	N (elements)	N_e	D(nm^{-3})	τ (ps)
H_1	1	0.159	0.02755	0.5O(1), 0.5O(2), 1Cu(1)	37	1343	272
Pyra.	2	0.0346	0.005993	0.25O(2), 0.5O(3), 0.5Cu(2)	20.5	3421	107
Ba	2	0.2524	0.04374	0.25O(1), 0.5O(2), 0.5O(3), 1Ba	66	1509	242
H_2	1	0.1335	0.02314	1O(3), 1Cu(1)	37	1599	299
Y	1	0.1335	0.02314	1O(3)	47	2031	180

and densities are given in the sixth and seventh columns, respectively, with the calculated positron annihilation lifetime listed in the last column. These are calculated using Equation 4 in which $p = 0.367$, taken from Table I. Obviously, the calculated results are based on the simple supposition that all monovacancies, vacancies and pyramids are of similar behaviour and have the same value of p. The validity of the supposition will be discussed below.

4.3. Calculating τ_1

According to the first three values of lifetime listed in the last column of Table II, the weighted average of lifetime in the barium "room" is 194 ps. The experimental value of τ_1 is 195 ps, so they are very close. This "room" is stable and its lifetime is almost kept constant during hydrogenation. Even if H_1 is occupied by hydrogen, the number of electrons in it adds only one, and the change of its lifetime is indistinguishable. The intensity of τ_1 is about 80% of the total intensity of the positron annihilation lifetime. The volume of the barium "room" (73.3%) is about three-quarters of a cell volume, and 3/4 is close to 80%. Therefore, it is believed that the positron annihilation with lifetime τ_1 occurs in the barium "room" during hydrogenation.

4.4. Change of τ_2 during hydrogenation

As discussed above, positron annihilation with lifetime τ_2 should occur in the yttrium "room". If the crystal is perfect without any defects, in this model τ_2 may be expressed as the average of the two values of τ in the yttrium "room", i.e. $\tau_2 = (229 + 180)/2 = 205$ ps. At the beginning of hydrogenation, the measured value of $\tau_2 (= 298$ ps) is larger than the calculated one (205 ps). Thus there are defects in the crystal, and the defects may be in the form of "microvoids" with low electronic densities. They have larger τ and cause τ_2 to increase. During hydrogenation τ of the defects is reduced because they capture hydrogen and their electronic densities are increased.

Next, let us consider what has happened in the bivacancy of yttrium during hydrogenation. For the sake of convenience, the process of positron annihilation with lifetime τ_2 is divided into periods of AB, BC, CD, etc. as shown in Fig. 3. If two neighbouring H_2 are occupied by hydrogen during hydrogenation, a new monovacancy, named H_3, is formed, consisting of couples of hydrogen, yttrium and O(3) or O(4), as shown in Fig. 4. Its volume, electronic number and density are 0.276 unit cells (or 0.047 83 nm^3), 47.5 and 1027 nm^{-3}, respectively. The predicted lifetime of H_3 is 365 ps. In this case, the other monovacancy left in the yttrium "room" has a very short τ and is too short to be recorded.

In the period AB, with defects still retaining their large τ and with H_3 being formed, τ_2 increases rapidly from 298 ps to 420 ps. At point B, the concentration of hydrogen in the yttrium "room" reaches its highest value. During period BC, hydrogen is supposed to diffuse from H_2 to H_1 and then occupy sites H_1 where the concentration of hydrogen is lower. As a result, the quantity of hydrogen in H_2 is reduced and τ_2 also decreases. At point C, τ_2 has decreased to 230 ps, even smaller than the initial value of 298 ps at point A. This fact may be due to defects in YBCO absorbing hydrogen during period AC ($t = 1000$ min), and their electronic densities increasing. By supposing that the period of 1000 min is long enough for defects to absorb hydrogen and to approach the saturated state, contributions from defects in τ_2 can be neglected at the end of this period. At point C, $\tau_2 (= 230$ ps) is only a little higher than 205 ps that the yttrium "room" has. Thus there is still some hydrogen left in H_2 at point C. According to the values of τ_2 (365, 205 and 230 ps), we may estimate that 17% hydrogen is left in H_2 at point C. With the hydrogen concentration decreasing to the lowest value at point C, the occupation of hydrogen starts again, and this will be the period CD. At the end of this period, τ_2 increases to 356 ps, approaching 365 ps, the lifetime H_3 has. At point D the contribution from defects is small. In the period from D to E, the diffusion of hydrogen from H_2 to H_1 occurs once again. Whereas, the quantity of diffused hydrogen is much smaller than that at the beginning time, at point E, 91% of sites H_2 are still occupied by hydrogen. The processes, occupation–diffusion–occupation–etc., are repeated again and again until equilibrium is obtained.

5. Conclusion

The behaviour of hydrogenation in YBCO may be interpreted by the above model: hydrogen occupies sites H_1, H_2 and H_3; for positron annihilation, process τ_1 occurs in the "room" where barium locates, and τ_2 follows the repeating process of hydrogen occupation–diffusion, until equilibrium.

According to the model, there is half a site for H_1 and half for H_3 and one site for H_2 in each unit cell. The maximum of values of H_1, H_2 and H_3 occupied by hydrogen are 0.5, 1 and 0.5, respectively. Thus, the total probability of occupation is 2. This coincides with experimental results [8]. The ratio of occupied probabilities between H_1 and $H_2 + H_3$ is 1/3. In Fig. 1, the ratio of intensities between H_2O and CH_3 is about 1/4. They generally conform with each other.

Acknowledgements

W. M. C. thanks Ms X. H. Wang for reading and revising this paper. This work was supported by the Chinese National Centre for Research and Development on Superconductivity.

References

1. J. J. REILLY, M. SUENAGA, J. R. JOHNSON, P. THOMPSON and A. R. MOODENGAUGH, *Phys. Rev. B* **36** (1987) 5694.
2. M. NICOLAS, J. N. DAOU, I. VEDEL, P. VAJDA and J. P. BURGER, *Solid State Commun.* **66** (1988) 299.
3. K. MORIMOTO, W. YE, S. ORIMO, T. TAKABATAKE, H. FUJII and T. HIHARA, *ibid.* **71** (1989) 291.
4. W. YE, T. TAKABATAKE, T. EKINO, T. TAMEGAI and H. FUJII, *Springer Proc. Phys.* **60** (1992) 299.

5. C. C. LAM, L. W. SHAO, X. JIN, W. M. CHEN, H. Q. XIONG, J. FENG, S. R. QI and K. C. HUNG, *Physica C* **270** (1996) 333.
6. K. MORIMOTO, T. TAKABATAKE, W. YE, S. ORIMO, T. HIHARA and H. FUJII, *ibid.* **159** (1989) 849.
7. H. FUJII, T. TAKABATAKE, W. YE, S. ORIMO and H. FUKUBA, *Jpn J. Appl. Phys.* **27** (1988) L525.
8. G. DORTMANN, J. ERXMEYER, S. VLAESSER, J. STEIGER, T. PAATSCH and A. WEIDINGER, *Phys. Rev. B* **49** (1994) 600.
9. W. M. CHEN, C. C. LAM, L. Y. LI, J. F. GENG, F. M. WU, K. C. HUNG and X. JIN, *J. Superconductivity* **9** (1996) 553.
10. W. M. CHEN, C. C. LAM, J. F. GENG, L. Y. LI, K. C. HUNG and X. JIN, *Physica C* **270** (1996) 155.
11. A. I. NAZZAL, V. Y. LEE, E. M. ENGLER, R. D. JACOWITZ, Y. TOKURA and J. B. TORRANCE, *ibid.* **153–155** (1988) 1367.
12. U. GONSER, "Microscopic Methods in Metal" (Springer, Berlin, 1986) pp. 249–96.
13. O. E. MOGENSEN, "Positron Annihilation in Chemistry" (Springer, Berlin, Heidelberg, 1995) pp. 55

Received 9 June 1997
and accepted 22 April 1998